Journal of Non-Crystalline Solids 354 (2008) 5386–5394

Contents lists available at ScienceDirect

Journal of Non-Crystalline Solids

journal homepage: www.elsevier.com/locate/jnoncrysol

Crystal growth kinetics in cordierite and diopside glasses in wide temperature ranges

Stefan Reinsch [a,*], Marcio Luis Ferreira Nascimento [b], Ralf Müller [a], Edgar Dutra Zanotto [b]

[a] Federal Institute for Materials Research and Testing, 12205 Berlin, Germany
[b] Vitreous Materials Laboratory, Department of Materials Engineering, Federal University of São Carlos, 13595-905 São Carlos-SP, Brazil

ARTICLE INFO

Article history:
Received 11 April 2008
Received in revised form 1 September 2008
Available online 17 October 2008

PACS:
81.05.Kf
81.10.−h
81.10.Aj

Keywords:
Crystal growth
Oxide glasses
Silicates

ABSTRACT

We measured and collected literature data for the crystal growth rate, $u(T)$, of μ-cordierite ($2MgO \cdot 2Al_2O_3 \cdot 5SiO_2$) and diopside ($CaO \cdot MgO \cdot 2SiO_2$) in their isochemical glass forming melts. The data cover exceptionally wide temperature ranges, i.e. 800–1350 °C for cordierite and 750–1378 °C for diopside. The maximum of $u(T)$ occurs at about 1250 °C for both systems. A smooth shoulder is observed around 970 °C for μ-cordierite. Based on measured and collected viscosity data, we fitted $u(T)$ using standard crystal growth models. For diopside, the experimental $u(T)$ fits well to the 2D surface nucleation model and also to the screw dislocation growth mechanism. However, the screw dislocation model yields parameters of more significant physical meaning. For cordierite, these two models also describe the experimental growth rates. However, the best fittings of $u(T)$ including the observed shoulder, were attained for a combined mechanism, assuming that the melt/crystal interface growing from screw dislocations is additionally roughened by superimposed 2D surface nucleation at large undercoolings, starting at a temperature around the shoulder. The good fittings indicate that viscosity can be used to assess the transport mechanism that determines crystal growth in these two systems, from the melting point T_m down to about T_g, with no sign of a breakdown of the Stokes–Einstein/Eyring equation.

© 2008 Elsevier B.V. All rights reserved.

1. Introduction

Crystal growth kinetics in glass forming liquids has been extensively studied and reviewed elsewhere [1–5]. For isochemical or polymorphic crystallization, the crystal growth rates have been described in terms of standard models of interface-controlled growth (see, e.g., [6–8]) such as *normal growth*, *screw dislocation growth* or *2D surface nucleated growth*. Detailed studies of crystal growth mechanisms are known for various glass forming compositions, such as SiO_2 and GeO_2 (normal growth) [9,10], $Na_2O \cdot 2SiO_2$ (screw dislocation) [11] and $K_2O \cdot 4B_2O_3$ (2D nucleated growth) [12]. However, in most studies the inferred crystal growth mechanisms are typically restricted to temperature ranges near the melting point, T_m, or somewhat above the glass transformation temperature, T_g, where crystal growth rates can be most easily measured.

In one of the first studies of crystal growth in glasses in *wide* temperature ranges, Burgner and Weinberg [13] analyzed the growth rates of internally nucleated lithium disilicate crystals in isochemical $Li_2O \cdot 2SiO_2$ glass forming melts between the glass transition temperature, T_g, and the melting point, T_m. Their analysis suggested that different governing growth mechanisms may be active for distinct temperature ranges, and that the usual phenomenological models could be applicable only for limited temperature ranges.

Meanwhile, crystal growth rate data for other two silicate glasses, cordierite and diopside, have also been measured in similarly broad temperature ranges. Thus, the extensive studies of surface nucleated, isochemical crystallization of high-quartz solid solution crystals, denominated "*μ-cordierite*" ($2MgO \cdot 2Al_2O_3 \cdot 5SiO_2$), in cordierite glasses reported in Refs. [14–21] allow a similar analysis. Some of these studies were part of a cooperative effort of the *TC* 7 Committee of the International Commission on Glass [22], which's aim was to advance the understanding of surface crystallization phenomena. Herein, numerous glasses close to the stoichiometric cordierite composition were melted in different laboratories and crystal growth experiments were conducted over a long period of time covering various experimental conditions.

As another case of surface nucleated crystallization, the crystal growth rates of *diopside* ($CaO \cdot MgO \cdot 2SiO_2$) in isochemical melts have also been comprehensively studied. Thus, crystal growth rate data are known for diopside glasses between 750–1155 °C and 1277–1378 °C [14,23–27]. In addition, thermodynamic and kinetic data, such as melting enthalpy and viscosity as a function of temperature are available for both systems, which facilitate quantitative comparisons between theory and experiment.

The objective of the present work is thus to summarize all measured growth rate data for μ-cordierite and diopside crystals in

* Corresponding author. Tel.: +49 30 6392 5950; fax: +49 30 6392 5976.
E-mail address: stefan.reinsch@bam.de (S. Reinsch).

0022-3093/$ - see front matter © 2008 Elsevier B.V. All rights reserved.
doi:10.1016/j.jnoncrysol.2008.09.007

their isochemical liquids in wide temperature ranges, then to analyze and discuss their observed temperature dependencies in terms of the classical crystal growth models. We also present a proposal using combined growth mechanisms to explain the shoulder in the crystal growth curve of μ-cordierite.

2. Experimental

2.1. Samples

2.1.1. Cordierite glasses

Most of the data for the crystal growth rates of μ-cordierite refer to glasses having the nominal composition of cordierite (in wt%): 51.3 SiO_2, 34.9 Al_2O_3 and 13.8 MgO. In this work and in Refs. [14,15,19] cordierite glasses were melted from reagent grade MgO and Al_2O_3 (both from Merck) and SiO_2 (quartz sand, Walbeck GmbH, Weferlingen) at 1590 °C in air for at least 8 h in Pt-crucibles. Meltings of 500 ml batches were carried out in conventional electric furnaces and in medium frequency inductive furnaces (4*l* batches). In the latter case, glass homogeneity was improved by stirring. Diaz-Mora et al. [20,21] used two cordierite glasses from Schott Glaswerke: one glass (B9455) had the nominal cordierite composition; another (GM30870) had 14.6 MgO, 33.2 Al_2O_3, 52.3 SiO_2 wt%. Yuritsyn et al. [16,17] used stoichiometric cordierite glasses melted from chemically pure $Al(OH)_3$, $MgCO_3$ and $SiO_2 \cdot n$-H_2O in Pt/Rh crucibles at 1600 °C for 4 h. All compositions are summarized in Table 1.

In this work and Refs. [14,15,19], glass plates of $\approx 10 \times 15 \times 1$ cm^3 were prepared by casting the melts onto steel plates and slowly cooling to room temperature from 750 °C. Wet chemical analysis of the quenched glasses showed that no oxide component deviates more than 0.8 wt% from the nominal composition. The water content determined by hot vacuum extraction and IR spectroscopy [28] for one of the glasses was 0.033 mol/l (226 wt ppm).

2.1.2. Diopside glasses

The diopside glasses reported by several authors [14,23–27,29–34] and that used in the present study were melted in air in Pt crucibles. In this work and Ref. [14], glass plates of $\approx 10 \times 15 \times 1$ cm^3 were splat cooled onto steel plates and slowly cooled to room temperature from 740 °C. Briggs and Carruthers [23] made an X-ray fluorescence analysis confirming that the composition of their glass was very close to the nominal composition, and was free of iron, titanium and alkali metal oxides, but had 0.25 mol% Al_2O_3. Nascimento et al. [25] used the ICP technique for chemical analysis, which showed that his glass composition deviates less than 1 wt% from the diopside stoichiometry. Reinsch [14] used a diopside glass with addition of 1 wt% Al_2O_3. Chemical analysis of this glass (19.7 MgO, 25.8 CaO, 54.5 SiO_2, 1 Al_2O_3 wt%) showed that no oxide component deviate more than 1 wt% from the nominal composition. The water content measured by hot vacuum extraction was 0.12 mol/l (758 wt ppm) [28]. Zanotto [27] used also a diopside glass with 1 wt% Al_2O_3. Kirkpatrick et al. [24] analyzed their glass with an electron microprobe, indicating a composition of 19.1 MgO, 26.4 CaO, 56.2 SiO_2 wt%, thus having only a minor discrepancy from the nominal diopside composition. Unfortunately, however, impurity and water contents were not always reported, but all these glasses have small departures from the stoichiometric diopside (18.61 MgO, 25.9 CaO, 55.49 SiO_2 wt%). All compositions are summarized in Table 1.

Table 1
Composition of all glasses used for crystal growth measurements in wt%

Cordierite glasses	SiO_2	MgO	Al_2O_3	Impurities
Cordierite	51.3	13.8	34.9	
This work and [13,14,18]	51.3 ± 0.8	13.8 ± 0.8	34.9 ± 0.8	
Yuritsin [15,16]	51.85	12.82	34.62	0.39 CaO/0.33 Na_2O
Diaz-Mora [19,20]	52.3	14.6	33.2	
Diopside glasses	**SiO_2**	**MgO**	**CaO**	**Al_2O_3**
Diopside	55.49	18.61	25.9	
This work and Reinsch [13]	54.55	19.72	25.80	1.02
Nascimento [24]	55.5 ± 1	18.6 ± 1	25.9 ± 1	
Briggs [22]	55.49	18.61	25.9	0.25 mol%
Zanotto [26]	54.96	18.4	25.64	1
Kirkpatrick [23]	56.2	19.1	26.4	

2.2. Measurements

2.2.1. Viscosity

In the present work, the viscosities of cordierite and diopside melts were determined by complementary methods. T_g was determined by a horizontal dilatometer (heating rate 5 K/min, Netzsch 402 E). Beam bending viscometry (heating rate 5 K/min, BAM) was used for the range $\log_{10}(\eta/(\text{Pa s})) = 12.3 - 9$ and for $\log_{10}(\eta/(\text{Pa s})) < 5$ ($T > 1000$ °C) rotational viscometry (BAM, measuring head Haake VT550) was applied.

The viscosity of the cordierite melt was also measured by Giess and Knickerbocker [35] at 900 and 920 °C with a parallel plate viscometer. Yuritsyn et al. obtained T_g data by means of dilatometry [16]. The viscosity of the diopside melt was measured by Licko and Danek [29] in an oscillating viscometer using a platinum–rhodium crucible and a cylinder with conical end. Nascimento et al. [25], Kozu and Kani [30] and McCaffery et al. [31] used a rotation viscometer. Sipp et al. [33] measured η by a compression method. Taniguchi [34] applied the counterbalanced method with Pt body and crucible, and the fiber elongation method. And finally, Neuville and Richet [32] did not disclose the technique used in their work.

2.2.2. Crystal growth rate

2.2.2.1. μ-Cordierite. Crystal growth rate measurements were performed using bulk pieces of glass ($\approx 5 \times 5 \times 5$ mm^3) with fractured, polished, or SiC ground surfaces in the present study as well as in Refs. [14–21]. Most of the thermal treatments were performed in air with ≈20% relative humidity (dew point ≈8.5 °C). The influence of the ambient water vapor pressure was checked by crystal growth experiments in argon/air atmospheres of different humidity [14,36] (dew point = −60 to 25 °C). Different techniques were used to measure the crystal growth rates of μ-cordierite at low and high temperatures. Below 830 °C we measured the growth of pre-existing crystals by electron or optical microscopy (increase of the maximum radius of selected surface crystals). Between 830 and 920 °C the maximum radius of crystals grown during one-step crystallization treatments were measured. Above 1000 °C we measured the thickness of the crystalline surface layer. Between 900 and 1050 °C both methods were used.

Isothermal treatments at 830–1100 °C were carried out in a conventional laboratory furnace. The samples were driven into the hot furnace using a platinum thermocouple as the sample holder. In other cases, annealing steps were made in a quartz glass tube furnace under controlled ambient conditions within a steel glove box. The accuracy of temperature measurement was ±10 K. Short time thermal treatments at high temperatures (1100–1350 °C) were performed in a specially designed vertical corundum tube furnace. The thermocouple and the platinum specimen holder were quickly moved along the tube axis where a linear gradient of 20 K/cm between 300 and 1500 °C was maintained. Due to the small heat capacities of small samples and the platinum holder, very high heating rates, up to about 1200 K/min, at least in the vicinity of the glass surface were attained. An empty sample holder

reached thermal equilibrium within 10 s. We measured the thickness of the crystalline surface layer between 200 and 1100 μm using annealing times between 1 and 3 min to ensure thermal equilibrium at least within the near surface layer of the sample. Nevertheless, for these short time measurements we have to assume a higher inaccuracy than for the other measurements. It is not possible to quantify this inaccuracy because of the unknown thermal conductivity of our samples and the resulting influence on the measured crystal layer thickness. But, the error is likely not larger than 50%, which is twice the size of the used symbols in Fig. 2(a) still fully embedded within the present data scatter.

2.2.2.2. Diopside. Numerous crystal growth rate data for diopside glasses between 750–1155 °C and 1277–1378 °C are known from literature. For instance, Briggs and Carruthers [23] measured crystal growth rates from 900 to 1150 °C by hot stage microscopy. Zanotto [27] measured the growth rate at 820 °C. Reinsch ([14] and new measurements shown in this article) measured u from 750 to 1050 °C by optical microscopy and SEM on polished and fractured surfaces. Fokin and Yuritsyn [37] measured growth rates between 800 and 875 °C by optical microscopy using polished and fractured surfaces. Nascimento et al. [25] measured diopside crystals on fire polished surfaces at 913, 923 and 950 °C. Crystal growth rates at low undercoolings ($\Delta T = T_m - T \leqslant 115$ K) were determined by Kirkpatrick et al. [24] using a hot stage microscope.

2.3. Melting temperature

The melting temperature of diopside in its isochemical melt is T_m = 1397 °C [38]. T_m of the metastable μ-cordierite cannot be directly measured. Therefore, we assume that its upper bound is the melting point of the stable high temperature polymorph of cordierite, denoted as indialite, h- or α-cordierite, at 1467 °C [38]. The lower bound of T_m is assumed to be ≈ 1350 °C since metastable μ-cordierite is detectable as the primary crystal phase up to 1300 °C [19].

3. Results

3.1. Viscosity

Viscosity data for cordierite melts are shown in Fig. 1 (upper curve). Our data are combined with data of Giess and Knickerbocker [35] and Yuritsyn et al. [16]. The fitted VFTH curve for cordierite glass is given by Eq. (1a), where η is given in Pa s and T in K. The measured viscosity of our diopside melt and related literature data [25,27,29–34] are also shown in Fig. 1 (lower curve). The resulting average curve for diopside, by fitting all data, is given by Eq. (1b), with η in Pa s, and T in K. For any given temperature, the cordierite melt is more viscous than liquid diopside

$$\log_{10}(\eta/(\text{Pa s})) = -3.97 + 5316\ \text{K}/(T - 762\ \text{K}) \quad \text{(cordierite)}, \quad (1a)$$

$$\log_{10}(\eta/(\text{Pa s})) = -4.27 + 3961\ \text{K}/(T - 751\ \text{K}) \quad \text{(diopside)}. \quad (1b)$$

3.2. Crystal growth rates

Crystal growth rates of μ-cordierite in its isochemical melt, measured in this work (open circles in Fig. 2(a)) and in previous studies [14–21], and similar data for diopside, measured here (open circles in Fig. 2(b)) and in Refs. [14,23–25,27,37], are shown in Fig. 2(a) and (b), respectively. These collected data cover an exceptionally wide temperature range, i.e. 800–1350 °C (μ-cordierite) and 750–1378 °C (diopside). The maximum of $u(T)$ occurs at about 1250 °C for both glasses. A smooth shoulder is observed around 970 °C for μ-cordierite (arrow in Fig. 2(a)). For diopside, such a shoulder is much less pronounced and possibly hidden by the large data scatter in this temperature range. As expected from the viscosity curves, the crystal growth rates of diopside are somewhat higher than of μ-cordierite at any temperature. However, at their respective T_g ($10^{12.3}$ Pa s) the growth rate of diopside is about one order of magnitude lower than that of μ-cordierite.

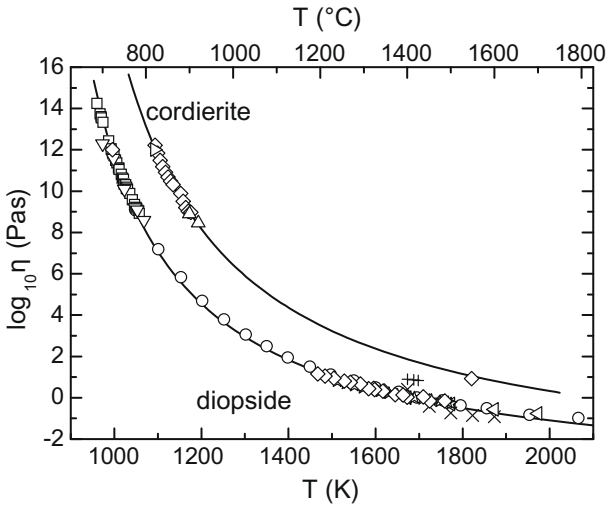

Fig. 1. Viscosity curves of cordierite and diopside liquids. Cordierite: ◇: this work; Δ: Giess et al. [35]; ▷: Yuritsin et al. [16]. Diopside: ◇, ✯: this work; o: Neuville et al. [32]; □: Sipp et al. [33]; +: Kozu and Kani [30]; ×: McCaffery et al. [31]; ▽: Taniguchi [34]; ◁: Licko and Danek [29]. Lines: Vogel–Fulcher–Tammann–Hesse (VFTH) fits for cordierite and diopside according to Eqs. (1a) and (1b), respectively.

3.2.1. Data scatter

Whereas for diopside, $u(T)$ data from different authors show remarkable similarity, significant scatter is evident for μ-cordierite. This scatter can be partially attributed to the decisive influence of humidity in different melts. This effect was measured in Refs. [14,36], where, e.g., u at 945 °C increased from 0.2 to 0.6 μm min^{-1} for increasing air humidity (dew points between −60 and +25 °C). The other important factor is that liquid diopside is much more depolymerised (has much more Q^2 units in NMR notation) than cordierite melt, thus its highly broken structure is not so sensitive to a few percent more or less impurities.

Another source of data scatter could be impurities and small departures of stoichiometry and the different techniques used to obtain crystal growth rate data, i.e. by measuring the dimension of separate crystals or the thickness of the crystalline surface layer. However, these two types of data are not significantly different, especially in logarithmic scale. This finding is illustrated for μ-cordierite in Fig. 3(a), where a large μ-cordierite surface crystal is growing from a pristine, vacuum-fractured glass surface (parallel to the paper plane). Its radius is comparable to the thickness of the μ-cordierite surface layer that grew perpendicularly from the sample surfaces (the latter surface was ground with SiC causing a high number density of surface crystals). Small deviations (a factor of two) due to the crystal orientation would not appear in the logarithmic scale of Fig. 2(a). Fig. 3(b) shows diopside crystals on a polished glass surface annealed in air at 830 °C for 210 min. Diopside crystals mainly appear as separately grown squares.

4. Data analysis

4.1. Basic equations

In terms of the standard crystal growth models, the interface-controlled crystal growth rate $u(T)$ is given by Eq. (2) [1,6], where

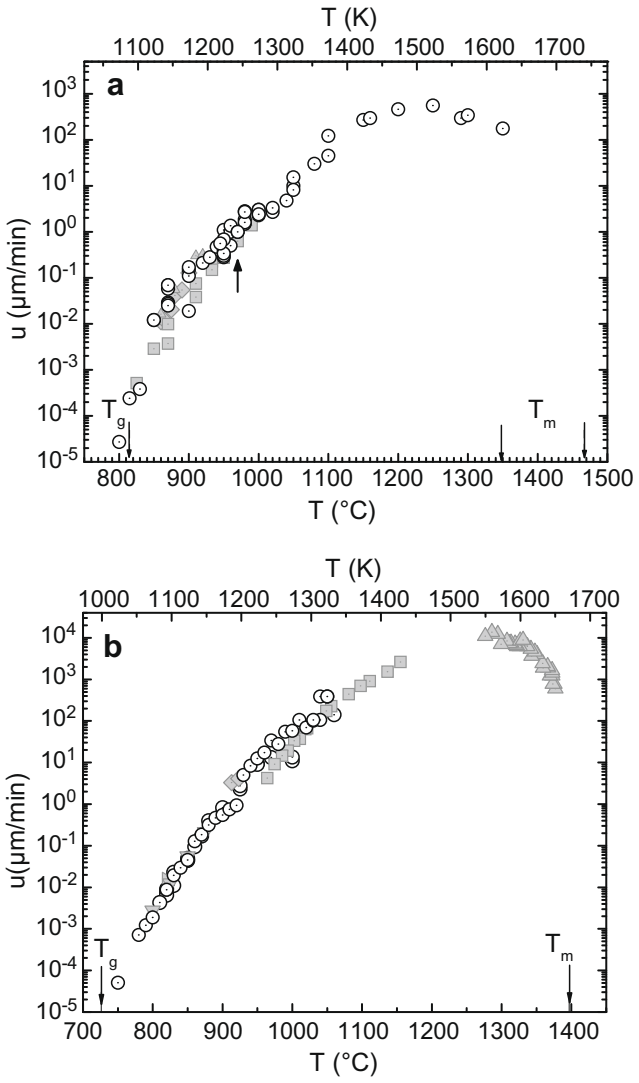

Fig. 2. (a) Crystal growth rate, *u*, of μ-cordierite in its isochemical liquid *vs.* temperature, *T*. Points: ○: this work and [14,15,19]; □: Yuritsin [16,17]; ◇: Hanay [18]; Δ: Diaz-Mora [20,21]. (b) Crystal growth rate, *u*, of diopside in its isochemical liquid *vs.* temperature, *T*. Points: ○: this work, [14]; ◇: Nascimento [25]; ▹: Zanotto [27]; Δ: Kirkpatrick et al. [24]; □: Briggs et al. [23]; ∇: Fokin [26]. Arrows indicate the dilatometric glass transition temperature, T_g, and the melting temperature, T_m. Possible upper and lower bounds for T_m according to 2.3 are indicated for metastable μ-cordierite in (a). The maximum error is about twice the size of the used symbols.

d in m is the size of the molecular building unit, $Z(T)$ is the attachment flow in $m^{-2}\,s^{-1}$, $f(T)$ is the fraction of preferred growth sites at the interface, $\Delta G(T)$ the bulk free energy change upon crystallization, *R* the gas constant, and *T* the absolute temperature

$$u(T) = d^3 \cdot Z(T) \cdot f(T) \cdot \left[1 - \exp\left(-\frac{\Delta G(T)}{RT}\right)\right], \tag{2}$$

d is estimated from the volume of a building unit according to Eq. (2a), where this building unit is set to the formula unit, V_m is its crystal molar volume, and N_A is the Avogadro number

$$d = \sqrt[3]{V_m/N_A}. \tag{2a}$$

$Z(T)$ is given by Eq. (3a) [7], where λ is the jump distance, $c \leqslant 1$ is a steric factor, and k_B is the Boltzmann constant. Eq. (3a) assumes that the molecular motion required for crystal growth is similar to that involved in shear viscous flow in the bulk liquid (Eyring assumption)

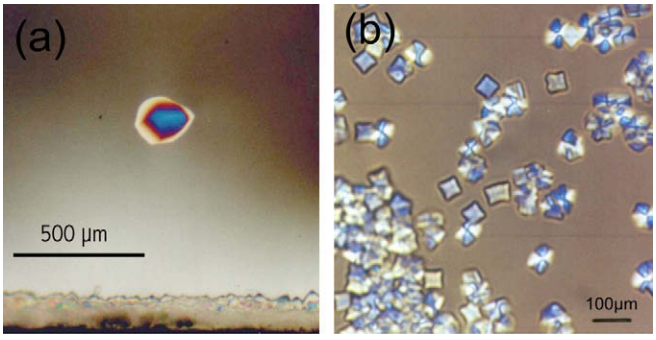

Fig. 3. (a) μ-cordierite crystal at a cordierite glass surface fractured and annealed in vacuum (980 °C, 30 min). A compact crystalline surface layer of μ-cordierite grew from SiC-ground surfaces of the sample. Transmitted light optical micrograph, top view, crossed nicols. (b) Diopside crystals at a polished diopside glass surface annealed in air (830 °C, 210 min). Transmitted light optical micrograph, top view, crossed nicols.

$$Z(T) = c\frac{k_B T}{d^3 \lambda^2 \eta(T)}. \tag{3a}$$

The first two terms in Eq. (2), $d^3 \cdot Z\,(T)$ in $m\,s^{-1}$, simplify to $d \cdot v$, where *v* is the jump frequency in s^{-1} defined by Eq. (3b) [2], when $c = 1$ and $d = \lambda$ are assumed. *b* in Eq. (3b) represents terms of weak temperature dependence

$$v(T) = \frac{k_B T}{d^3 \eta(T)} = b/\eta(T). \tag{3b}$$

For $f(T)$, the fraction of preferred growth sites, three phenomenological models are frequently used [1,2]. For *normal growth,* the crystal/melt interface is rough on atomic scale, i.e. almost every site allows the attachment of new building units, and $f(T) \cong 1$.

According to the *screw dislocation* model, the crystal/melt interface is smooth on atomic scale but plagued by screw dislocations. Growth takes place at step sites provided by screw dislocations intersecting the interface, and $f_s\,(T)$ is expressed by Eq. (4) [1,39], where σ is the specific surface energy of the melt-crystal interface, and c_s is a constant

$$f_s(T) = c_s \frac{d\Delta G(T)}{4\pi\sigma V_m}. \tag{4}$$

In the 2D *secondary surface nucleation growth* model, the surface is atomically smooth and free from defects. Growth occurs by formation of two-dimensional nuclei on the interface, followed by lateral growth, and $f_{2D}(T)$ is expressed by Eq. (5a) [1,7]

$$f_{2D}(T) = c_{2D} \exp\left(-\frac{W(T)}{k_B T}\right) = c_{2D} \exp\left(-\frac{(\pi d V_m \sigma^2)/\varepsilon \Delta G(T)}{k_B T}\right), \tag{5a}$$

where c_{2D} is a constant and $W(T)$ is the work of forming the critical 2D surface nucleus. Herein, $\varepsilon = 1$ denotes the *small crystal* case (layer by layer growth) and $\varepsilon = 3$ the *large crystal* case (multi-nucleus growth) [1,40]. The temperature dependence of f_{2D} is illustrated by Eq. (5b) representing all terms of weak temperature dependence by *B* according to Eq. (5c) [2]

$$f_{2D}(T) \propto \exp\left(-\frac{B}{T\Delta G(T)}\right), \tag{5b}$$

$$B = \frac{\pi d V_m \sigma^2}{\varepsilon k_B}. \tag{5c}$$

Furthermore, a *combined mechanism* is considered here. We assume that the melt/crystal interface, growing from screw dislocation defects, is additionally roughened by superimposed 2D surface nucle-

ation, particularly at large undercoolings. This situation is schematically illustrated in Fig. 4 and represented by Eq. (6). The constants c_s and c_{2D} were treated as freely adjustable with f_s, f_{2D} and $f_s + f_{2D} < 1$ is ensured. In this way, the normal growth model always yields the maximum values of $u(T)$

$$f_c(T) = f_s(T) + f_{2D}(T). \tag{6}$$

Finally, the bracket in Eq. (2) gives the occupation probability of growth sites, which depends on $\Delta G(T)$, the bulk free energy change upon crystallization. $\Delta G(T)$ can be approximated by Eq. (7a) for small undercoolings, $\Delta T = T_m - T$, and by Eq. (7b) for wide temperature ranges $\frac{1}{2}T_m < T < T_m$, where T_m is the melting point of the crystal in its isochemical melt [1,7]. For binary alkali silicate glasses, Eqs. (7a) and (7b) were found to be accurate for small undercoolings only, giving for other cases only an upper and lower bound for ΔG, respectively,

$$\Delta G(T) = \frac{\Delta H_m \cdot \Delta T}{T_m}, \tag{7a}$$

$$\Delta G(T) = \frac{\Delta H_m \cdot \Delta T \cdot T}{T_m^2}. \tag{7b}$$

4.2. Estimation of crystal/melt interfacial energy

Uhlmann and Uhlmann[2] proposed a simple method to estimate the crystal/melt interfacial energy, σ. Expressing all the terms of weak temperature dependence in Eq. (2), by B (Eq. (5c)), b (Eq. (3b)), and C he wrote for the 2D *surface nucleated growth model*

$$u(T) = \frac{Cb}{\eta} \exp\left(-\frac{B}{T\Delta G(T)}\right) \tag{8}$$

or

$$\ln u\eta = \ln Cb - \frac{B}{T\Delta G(T)}. \tag{9}$$

Assuming B and Cb as constants, plots of $\ln(u\eta)$ versus $(T\Delta G)^{-1}$ should yield straight lines of negative slope B. σ can then be obtained from B according to Eq. (5c). σ is often represented in terms of α used in the Skapski–Turnbull expression [41]:

$$\alpha = \frac{\sigma}{\Delta H_m} \sqrt[3]{N_A V_m^2}. \tag{10}$$

For *μ-cordierite*, a plot of $\ln u\eta$ versus $(T\Delta G)^{-1}$ is shown in Fig. 5. Confirming previous $u(T)$ studies in wide temperature ranges [2,13], the experimental data cannot be fitted by a single set of parameters. At least, two straight lines with widely different slopes, B, might be fitted. Each B yields two values of σ according the small and large crystal case ($\varepsilon = 1$ or 3 in Eq. (5c)). The calculated values of σ and α are shown in Table 2. Due to the uncertain melting point of μ-cordierite (T_m = 1350–1467 °C), we considered ΔH_m = 175 and 190 kJ/mol for the lower und upper bound of T_m, respectively, both

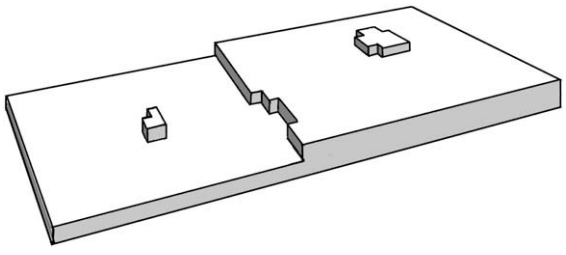

Fig. 4. Schematic illustration of the combined mechanism Eq. (6) assuming simultaneous crystal growth from screw dislocations (step) and from additional 2D surface nuclei at the spiral step planes.

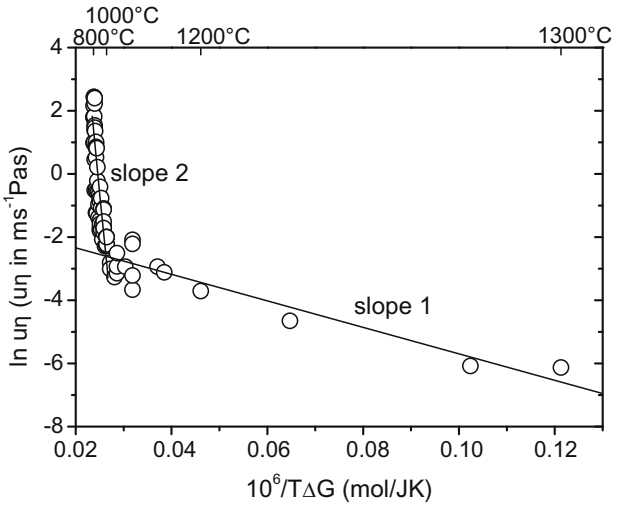

Fig. 5. Estimation of the liquid/crystal interfacial energy, σ, for μ-cordierite. $\Delta G(T)$ was calculated by Eq. (7b). σ was obtained from slope 1 and slope 2. Results are summarized in Table 2.

taken from [42]. The molar volume of the crystal building unit (one formulae unit) is $V_m = 22.59 \times 10^5$ m^3/mol [42]. Taking slope 1 (small undercoolings), α from the 2D nucleation-growth analysis is $0.06 < \alpha < 0.2$, which are lower than the well-known values derived from Classical Nucleation Theory (CNT) for several other silicate glasses ($0.4 < \alpha < 0.6$ [43,44]). Taking slope 2, α ranges between 0.36 and 1.07, i.e. not far from the expected range estimated from CNT, and could thus corroborate the 2D *surface nucleation* as the operative growth mechanism for this system for large undercoolings.

For *diopside*, a plot of $\ln(u\eta)$ versus $(T\Delta G)^{-1}$ is shown by Fig. 6. Surface energies σ and α obtained from the fitted slopes are given in Table 2 (ΔH_m = 138 kJ/mol [38], and $V_m = 6.61 \times 10^5$ m^3/mol). As for μ-cordierite, the growth rate data for diopside can be fitted by two straight lines with widely different slopes. The α values from slope 1 are $0.04 < \alpha < 0.07$, which are far below the well-known values derived from CNT, while α values from slope 2, $0.24 < \alpha < 0.75$, are mostly within the expected range estimated from CNT.

4.3. Direct fitting

Crystal growth mechanism and σ may also be inferred from a direct fitting, which can be performed by dropping the assumptions Cb = constant, with $d \approx \lambda$ (used in Figs. 5 and 6). The best fitting results are shown in Figs. 7 and 8, for μ-cordierite and diopside, respectively. We used Eqs. (1), (2), (3a) and (7b) with $f = 1$ for the *normal* growth model. For the *screw* dislocation model, f was calculated by Eq. (4). For the 2D *surface nucleation* model, f is set to Eq. (5a). In case of the *combined* mechanisms, both terms of f are superimposed according to Eq. (6). Due to the uncertain melting point of μ-cordierite $T_m \approx$ 1350–1467 °C [42] it was set to the bound values. The corresponding melting enthalpies ΔH_m = 175 and 190 kJ/mol were also taken from [42] assuming that the formulae unit ($2MgO \cdot 2Al_2O_3 \cdot 5SiO_2$; M = 585 g/mol) is the building unit. ΔH_m for diopside is ≈138 kJ/mol (formulae unit; M = 216 g/mol) [38].

For *μ-cordierite*, normal growth does not fit the experimental data, except at the lowest temperatures (n, dotted line in Fig. 7). This is confirmed by Jackson's treatment of the interface [45,46], which expects that materials with high entropy of melting, such as diopside ($\Delta S_m^d = \Delta H_m / RT_m \cong 10$) and cordierite ($\Delta S_m^c = \Delta H_m / RT_m \cong 13$), have smooth crystal/melt interfaces.

Table 2
Surface energy σ (mJ/m^2) and α obtained from different methods

System	Method	Mechanism	ε	T_m (°C)	σ_1	σ_2	α_1	α_2
μ-Cordierite	Uhlmann	2D	1	1467	70	372	0.12	0.62
			3	1467	122	644	0.2	1.07
			1	1350	34	204	0.06	0.36
			3	1350	58	353	0.10	0.63
					σ		α	
	Direct fitting	2D	3	1467	140		0.25	
		Screw	3	1350	224		0.40	
		Combined	3	1350	280		0.50	
Diopside	Uhlmann	2D (solid)	1	1397	42	435	0.04	0.43
			3	1397	73	754	0.07	0.75
		2D (dashed)	1	1397		236		0.24
			3	1397		408		0.41
					σ		α	
	Direct fitting	2D	3	1397	70		0.07	
		screw	3	1397	400		0.40	

$\varepsilon = 1$ small crystal case, $\varepsilon = 3$ large crystal case. If one changes ε from 1 to 3, the calculated σ and α change by a factor of $3^{1/2}$ (Eqs. (5c) and (10)). σ_i and α_i: obtained from slope i (1 or 2).

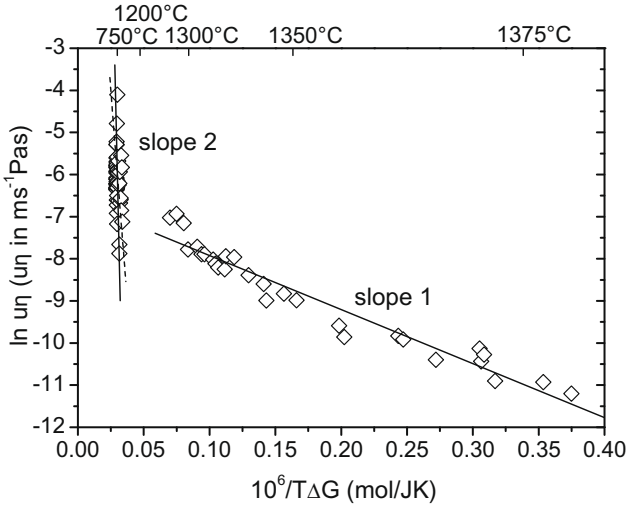

Fig. 6. Estimation of the liquid/crystal interfacial energy, σ, for diopside. $\Delta G(T)$ calculated by Eq. (7b). σ was obtained from slope 1 and slope 2. The dashed line (slope 2) indicates the uncertainty of slope determination. Results are summarized in Table 2.

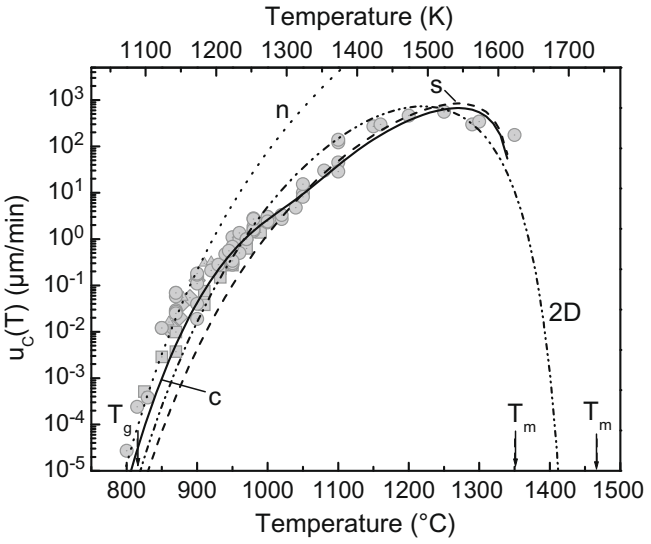

Fig. 7. Best fits of crystal growth rate data for μ-cordierite: Normal growth: n, dotted line; screw dislocation: s, dashed line; 2D surface nucleated growth: 2D, dashed-dotted line, combined mechanism: c, solid line. Calculation parameters are summarized in Table 3. Experimental points: see Fig. 2(a).

Using the screw dislocation model, the experimental data above 1000 °C can be fitted when $T = 1350$ °C is assumed. The results (not shown) for higher T_m are much worse. For $T < 1000$ °C the deviation from the experimental points is up to one order of magnitude. If $T_m = 1467$ °C is used, the 2D surface nucleated growth model also fits the experimental points fairly well (2D, dashed-dotted line in Fig. 7). But in the low temperature range ($T < 900$ °C) a deviation of about one order of magnitude occurs. The best fit is obtained using the combined mechanism. It is possible to fit the smooth shoulder in $u(T)$ at 970 °C and its temperature dependence below 900 °C with $\sigma = 280$ mJ/m^2 (see Table 2) and $T_m = 1350$ °C (c, solid line in Fig. 7). This fit required a high value of c_{2D} compensating the low value of the exponent in Eq. (5a) at the temperature range of the observed shoulder in $u(T)$. Only this way, $f_{2D} \gg f_s$ and a pronounced shoulder could be attained.

For *diopside,* all three growth models are more or less applicable when independently fitted. Thus, the normal growth model (n, dotted line in Fig. 8) fits the experimental points up to 1150 °C. However, we had to assume a small steric factor $c = 0.04$ notwithstanding the used values of $c = 1$ for all other models. Using $c = 1$ for normal growth results in a more than one order of magnitude higher $u(T)$. With the screw dislocation model (s, dashed line in Fig. 8) as well as with the 2D model (2D, dashed-dotted line in Fig. 8), the experimental data can be well fitted within the whole temperature range. However, for the latter model this fitting is only possible assuming a very low α (see Table 2). Fitting in terms of the combined mechanism was also possible requiring a high value of c_{2D}, too (not shown).

5. Discussion

5.1. Crystal growth mechanism

Two methods of assessment of the crystal growth mechanism were applied here for *μ-cordierite*: direct fitting of crystal growth and estimation of crystal/melt interfacial energy. With direct fitting, both the 2D-surface nucleation and the screw dislocation growth model could be fitted with sufficient accuracy. These assessment uncertainties may arise from the unknown value of T_m or from the experimental difficulties to measure the very large

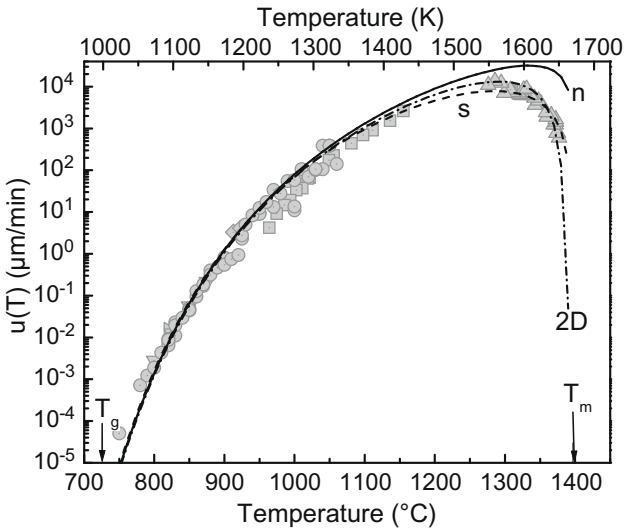

Fig. 8. Best fits of crystal growth rate data for diopside. Normal growth: n, dotted line, screw dislocation: s, dashed line, 2D surface nucleated growth: 2D, dashed and dotted line. The used parameters are summarized in Table 4. Experimental points: see Fig. 2(b).

$u(T)$ of μ-cordierite in the high temperature range (small undercoolings). For small undercoolings, the value of σ obtained from slope 1 in Fig. 5 (see Table 2), assuming the 2D mechanism, have little physical meaning. For large undercoolings, Fig. 5 more convincingly indicates the 2D surface nucleation mechanism since the resulting σ has a more significant physical meaning. In the direct fitting (Fig. 7), the 2D-mechanism best fits $u(T)$. Very best fits are obtained assuming that 2D-surface nucleation additionally roughens the spiral steps (combined mechanism).

A more defined situation is observed for *diopside*. For small undercoolings, Kirkpatrick [24] indicated the spiral growth mechanism. Confirmingly, very small values of α (<0.07) of questionable physical meaning are found in Fig. 6 if the 2D surface nucleation mechanism is supposed. For large undercoolings, however, the 2D mechanism is more probable, since it yields physically meaningful σ. Accordingly, Kirkpatrick [8] also indicated that growth occurs by a surface nucleation mechanism at large undercoolings. In the direct fitting, the 2D and the spiral growth model give almost the same result. Fitting in terms of the combined mechanism was also possible (not shown).

Direct fitting of crystal growth and estimation of crystal/melt interfacial energy for both cases indicate that the fraction of preferred growth sites increases at large undercoolings, e.g. due to a change from the screw dislocation to the 2D nucleation growth mechanism.

5.2. Fitted parameters

The full and reduced energy parameters, σ and α, respectively obtained from the two methods used here are summarized in Table 2. Uhlmann's method assuming the 2D surface nucleation mechanism yields values which are too small for small undercooling (slope 1) if compared with well-known values from Classical Nucleation Theory for measurable homogeneous nucleation in silicate systems, which usually varies between 0.4 and 0.6 [43,44]. Slope 2 (large undercooling), which refers to temperatures near the respective shoulder and below yields reasonable α values for both systems. α values obtained from direct fitting for μ-cordierite are plausible for the screw dislocation and the combined mechanism. This finding also holds for diopside.

σ and α summarized in Table 2 show a large scatter. This scatter may arise from the uncertain validity of adopted assumptions concerning the growth mechanism, the small or large crystal case, the constancy of Cb, the applicability of Eq. (7b), and the uncertain melting point of μ-cordierite. Other small effects arise from the uncertain molar mass of the building unit, which is simply set to the formulae unit. At least for cordierite, which formulae unit contains five silica and four alumina tetrahedra, this is questionable [42] (please note that altering M will affect d, ΔH_M and ΔG).

All these uncertainties indicates that one should not trust any of the such-wise obtained results for σ and that the application of any method for estimating σ, particularly from $u(T)$ data restricted to narrow temperature ranges, could be misleading.

The mean jump distance, λ, is frequently assumed to equal d. For μ-cordierite, it was not possible to directly fit the experimental points with this assumption. Only for a significantly smaller λ, an acceptable fitting was possible (see Table 3). Thus, we used the jump distance λ as a free fitting parameter in Eq. (3a), whereas d was calculated with Eq. (2a). To perform a good fitting, even at low temperatures, near T_g, a somewhat lower λ than the oxygen ion radius ($\lambda \approx 0.13$ nm) was necessary. For diopside, good fitting with $\lambda = d$ was possible (see Fig. 8 and Table 4). But as we discussed for the estimation of σ, the fitted λ should only give an order of magnitude for the jump distance or the size of the jumping molecules.

5.3. Crystal growth rate shoulder

Most intriguing, a smooth shoulder appears at ≈970 °C for μ-cordierite and may be also present for diopside (but it is quite small and could be hidden by the data scatter). The best fitting of

Table 3
Parameters used for calculating crystal growth rates of μ-cordierite (curves in Fig. 7)

Parameter μ-cordierite		Normal growth	Screw dislocation	2D surface nucleated growth	Combined mechanism
M (g/mol)	+	585	585	585	585
T_m (°C)		1467	1350	1467	1350
λ (Å)	+	0.7	0.7	0.7	0.7
d (Å)	Eq. (2a)	7.21	7.21	7.21	7.21
c	+	1	1	1	1
α	Eq. (10)	–	0.4	0.25	0.5
σ (J/m^2)	#	–	0.224	0.140	0.280
c_S	#	–	0.5	–	0.5
c_{2D}	#	–	–	25	3×10^9

'+' parameter generally set to a uniform value (e.g. M to one formulae unit) and '#' parameter was adjusted.

Table 4
Parameters used for calculating crystal growth rates of diopside (curves in Fig. 8)

Parameter diopside		Normal growth	Screw dislocation	2D surface nucleated growth
M (g/mol)	+	216	216	216
T_m (°C)		1397	1397	1397
λ (Å)	+	4.79	4.79	4.79
d (Å)	Eq. (2a)	4.79	4.79	4.79
c	#	0.04	1	1
α	Eq. (10)	–	0.4	0.07
σ (J/m^2)	#	–	0.4	0.07
c_s	#	–	1	–
c_{2D}	#	–	–	0.05

'+' parameter generally set to a uniform value (e.g. M to one formulae unit) and '#' parameter was adjusted.

$u(T)$ including this shoulder was possible assuming that the melt/crystal interface, growing from screw dislocation defects, is additionally roughened by superimposed 2D surface nucleation, particularly at large undercoolings (Fig. 4). The possibility that different crystal growth mechanisms operate in a wide temperature range has been discussed by Burgner et al. [13] in their study of LS_2 glass. A possible change from screw dislocation to surface nucleated growth with increasing undercooling was also addressed by Gutzow et al. [1] for systems with intermediate $\Delta S_m/R$. The value of this parameter is large for the present glasses if the building unit is equated to the formulae unit. Computer simulations showed that, depending on the crystallographic orientation, atomic roughness can increase significantly with increasing $\Delta G/RT$, i.e., with increasing undercooling [47].

Thus, this supposition might be feasible, although no clear evidence can be claimed from the present study. Instead, several possibilities must be considered to account for this phenomenon, which may also affect the assessed growth mechanism and fitted parameters.

5.4. Model applicability

5.4.1. Chemical composition

The applicability of the applied standard model is restricted to interface-controlled isochemical crystal growth, which we assume to be valid for both glasses studied here. And, indeed, the linearity of the crystal size *versus* time curves, expected for such case, was verified for μ-cordierite between 920 and 1080 °C [15], and for diopside from 750 up to 850 °C [14]. The attained good fitting of $u(T)$ in the wide temperature range covered here also indicates the applicability of standard growth models.

Nevertheless, small effects like the observed shoulder in $u(T)$ might be affected by temporary changes of the chemical composition of growing crystals with annealing time or temperature. Such compositional changes have been experimentally verified by Fokin et al. [48] and Roskosz et al. [49] in other silicate systems. Considering diopside, however, preliminary results of quantitative EDX analysis by SEM (crystallized layer heat treated at 890 °C for 16 h) showed no difference between the glass and crystal phase compositions [50]. Up to now, no such analysis was performed for cordierite. X-ray powder diffraction studies [51] have shown that the position of (101) peak of the X-ray powder diffraction trace of μ-cordierite (JCPDF 14-249) is at ≈0.346 nm up to 1080 °C. This observation indicates that the SiO_2 content of μ-cordierite is close to that of cordierite [52]. Beyond that temperature, however, compositional shifts cannot be excluded because μ-cordierite readily transforms to indialite (JCPDF 21-549), the high temperature polymorph of cordierite [53]. The latter dominates the overall crystallization of cordierite glasses above 1000 °C. Nevertheless, it was shown in Ref. [54] that on heating the glass first transforms to μ-cordierite, and then to indialite. Thus, even the growth of a thick surface layer, which is mainly composed of indialite, is controlled by a thin 'front-layer' of μ-cordierite. In Ref. [19] this mechanism was observed to occur up to 1300 °C by X-ray experiments.

5.4.2. Crystal morphology

For diopside, morphology changes have not been exhaustibly tested, and to the best of our knowledge there is no published evidence about changes in crystal morphology with time or temperature. Recently, however, Fokin [50] communicated two distinct morphologies, with different growth rates, growing on polished surfaces of a stoichiometric diopside glass at ≈800 °C, but these data must yet be confirmed by more detailed experiments.

For μ-cordierite, Diaz-Mora [21] observed a change in morphology from elongated hexagonal crystals to regular hexagons at $T < 900$ °C. Changes in morphology were also reported in Ref. [51]. Small crystals <2 μm, grown at $T < 900$ °C show cellular melt/crystal interfaces, whereas large crystals grown at $T > 1000$ °C are dendritically structured. Nevertheless, the shape of isolated crystals does not deviate from hexagonal bi-pyramids and their growth rate does not explicitly depend on time (or crystal size). Hence, we believe that the influence of morphology may be neglected for the measured crystal growth rate data of μ-cordierite.

5.4.3. Crystal surface roughness

$u(T)$ will increase by a transition from the small to the large crystal case if crystal growth is governed by 2D surface nucleation (Eq. (5a)). This might explain the change of slopes in Figs. 5 and 6. For μ-cordierite (Fig. 5), the ratio between slope 2 and slope 1 is 37 and 27 for $T_m = 1350$ °C and $T_m = 1467$ °C, respectively. For diopside (Fig. 6), this ratio is 106 (solid line) or 31 (dashed line). According to Eqs. (5a) and (5c), however, this ratio should be only 3. Therefore, this enormous change of slope is not due to a transition from small to large crystal growth. A transition from the small to the large crystal case might also explain the shoulder in $u(T)$ of μ-cordierite. Thus, we recalculated curve 2D in Fig. 7 (large crystal case) for the small crystal case (not shown in Fig. 7). The curves did not differ by more than ≈ 2.

5.4.4. Decoupling

Another possible explanation for the shoulder might be attributed to a possible breakdown of the Stokes–Einstein/Eyring equation (see Eq. (3b)). For instance, a recent study [55] demonstrates that below the glass transition temperature atomic motion through a metallic glass involves single-atom hopping, whereas motion above T_g is more collective. Similar findings have been reported for some organic liquids. For such fragile systems a substantial change in the diffusion mechanism seem to occur at temperatures about $1.2T_g$, and this temperature has been denominated decoupling temperature T_d. But, this phenomenon has not yet been firmly demonstrated for oxide glasses. Here, we should stress that the weak shoulder in Fig. 7 occurs at $\approx 1.2T_g$, where decoupling is expected. However, the inflection is too faint and uncertain to really demonstrate decoupling. For instance, one expects that for real decoupling – such as those reported in Ref. [55] below T_d, the Stokes–Einstein/Eyring equation would not describe the diffusion coefficients any longer, but here they do. In other words, decoupling leads to a permanent change in slope and not only to a kink in the crystal growth rate curves.

5.4.5. Temperature at the liquid/crystal interface

A further precondition for the accuracy of the crystal growth analysis is that the temperature of liquid/crystal interface equals that of the bulk specimen. Herron and Bergeron [56] suggested and successfully tested empirical equations to estimate the liquid/crystal interface temperature ΔT_i for temperatures near the maximum crystal growth rate u_{max} and at $u < 0.67\, u_{max}$ [25]. In order to check the related potential influence on $u(T)$, we used Herron and Bergeron's equation,

$$\Delta T_i = 17.12(u_{max}\Delta H_m)^{0.486}, \tag{12}$$

where u_{max} is in (cm/s) and ΔH_m in (cal/cm^3), to correct our $u(T)$ data with respect to temperature. For cordierite and diopside these corrections are at the most 5 and 50 °C, respectively, in the range of maximum growth rate. Hence, they could, in principle, exert a significant effect on the kinetic analysis of diopside. Such corrected $u(T)$ data were used to repeat the data analysis in Fig. 6, but calculations performed with and without them demonstrate that the main conclusions would not change.

6. Conclusions

We have analyzed crystal growth rate data of μ-cordierite and diopside crystals in their corresponding isochemical glass forming melts in a wide temperature range, from about T_g to T_m, with $u(T)$ varying by about 9 orders of magnitude. The maximum of $u(T)$ is reached at about 1250 °C in both systems. A weak shoulder in $u(T)$ is observed at 970 °C ($\sim 1.2T_g$) for μ-cordierite.

For diopside, the experimental $u(T)$ can be equally fit by the 2D surface nucleation growth mechanism and by the screw dislocation growth mechanism. However, the screw dislocation model yields parameters of more significant physical meaning.

For μ-cordierite, these two models also describe the experimental growth rates. However, the best fitting of $u(T)$, including the observed shoulder, was attained for a combined mechanism assuming that the melt/crystal interface, growing from screw dislocations, is additionally roughened by superimposed 2D surface nucleation at large undercoolings, starting at temperatures around the observed shoulder. Thus, this supposition might be feasible, although no clear evidence can be claimed from the present study.

Taken *in toto*, the experimental data could be fit within the whole temperature range by the standard dislocation growth model. The good fittings indicate that viscosity can be used to assess the transport mechanism that determines crystal growth in these systems, from the melting point T_m down to about T_g, with no sign of a breakdown of the Stokes–Einstein/Eyring equation. Similar findings were recently reported for pure silica glass [57].

Acknowledgments

MLFN would like to acknowledge DAAD (*Deutscher Akademischer Austauschdienst*) and the Brazilian agencies CAPES for financial support during his stay at BAM, and FAPESP for his postdoctoral fellowship (Grant 04/10703-0). EDZ thanks the Brazilian agencies Fapesp (Grant 07/08179-9) and CNPq for continuous support in the last 30 years. The authors thank I. Schubart for $u(T)$ measurements during his internship at BAM and Mark Ediger for a critical review of the manuscript.

References

[1] I. Gutzow, D. Kashchiev, I. Avramov, J. Non-Cryst. Solids 73 (1985) 477.
[2] D.R. Uhlmann, E.V. Uhlmann, in: M.C. Weinberg (Ed.), Ceramic Transactions Nucleation and Crystallization in Liquids and Glasses, vol. 30, American Ceramic Society, Westerville, OH, 1993, p. 109.
[3] W. Vogel, Glass Chemistry, Springer, Berlin, 1994.
[4] I. Gutzow, J. Schmelzer, The Vitreous State, Springer, Berlin, 1995.
[5] W. Hölland, G. Beall, Glass Ceramic Technology, Amer. Ceram. Soc., Westerville, OH, 2002.
[6] I. Gutzow, J. Cryst. Growth 42 (1977) 15.
[7] I. Gutzow, in: E. Kaldis, H.J. Scheel (Eds.), Crystal Growth and Materials, North-Holland, Amsterdam, 1977, p. 379. Chapter 1.11.
[8] R.J. Kirkpatrick, Am. J. Sci. 274 (1974) 215.
[9] M.L.F. Nascimento, E.D. Zanotto, Phys. Rev. B 73 (2006) 024209.
[10] P.J. Vergano, D.R. Uhlmann, Phys. Chem. Glasses 11 (2) (1970) 39.
[11] G.S. Meiling, D.R. Uhlmann, Phys. Chem. Glasses 8 (2) (1967) 62.
[12] C.J. Leedecke, C.G. Bergeron, J. Cryst. Growth 32 (1976) 327.
[13] L.L. Burgner, M.C. Weinberg, J. Non-Cryst. Solids 279 (2001) 28.
[14] S. Reinsch, Dr. Ing. thesis, Technical University of Berlin, 2001. (in German).
[15] T. Huebert, R. Mueller, M. Kirsch, Silikattechnik 39 (1988) 183 (in German).
[16] N.S. Yuritsyn, V.M. Fokin, A.M. Kalinina, V.N. Filipovich, Glass Phys. Chem. 20 (1994) 116.
[17] N.S. Yuritsyn, PhD thesis, St. Petersburgh, 1997 (in Russian).
[18] Ch. Hanay, Diploma Friedrich-Schiller University, 1992 (in German).
[19] R. Mueller, S. Reinsch, W. Pannhorst, Glastech. Ber. Glass Sci. Technol. 69 (1996) 12.
[20] N. Diaz-Mora, E.D. Zanotto, R. Hergt, R. Mueller, J. Non-Cryst. Solids 273 (2000) 81.
[21] N. Diaz-Mora, PhD thesis, Federal University of São Carlos, Brazil, 1994 (in Portuguese).
[22] W. Pannhorst, Ed., "Surface nucleation; Collection of selected papers published by the TC 7 members during their 10 years attempt to understand the nature of the active sites in surface nucleation" published by the Intern. Comm. on Glass (2000).
[23] J. Briggs, T.G. Carruthers, Phys. Chem. Glasses 17 (1976) 30.
[24] R.J. Kirkpatrick, G.R. Robinson, J.F. Hays, J. Geo. Res. 81 (1976) 5715.
[25] M.L.F. Nascimento, E.B. Ferreira, E.D. Zanotto, J. Chem. Phys. 121 (2004) 8924.
[26] V. Fokin, V. P. Klyuev, private communication.
[27] E.D. Zanotto, J. Non-Cryst. Solids 130 (1991) 217.
[28] R. Mueller, M. Gaber, P. Gottschling, Phys. Chem. Glasses 45 (2004) 85.
[29] T. Licko, V. Danek, Phys. Chem. Glasses 27 (2) (1986) 22.
[30] S. Kozu, K. Kani, Am. Ceram. Soc. Bull. 23 (10) (1944) 377.
[31] R.S. McCaffery, C.H. Lorig, I.N. Goff, J.F. Oesterle, O.O. Fritsche, AIME Techn. Publ. 100(1), 1932, p. 86.
[32] D.R. Neuville, P. Richet, Riv. Staz. Sper. Vetro 21 (6) (1990) 213.
[33] A. Sipp, Y. Bottinga, P. Richet, J. Non-Cryst. Solids 288 (2001) 166.
[34] H. Taniguchi, Contrib. Mineral. Petrol. 109 (1992) 295.
[35] E.A. Giess, S.H. Knickerbocker, J. Mater. Sci. Lett. 4 (1985) 835.
[36] R. Mueller, S. Reinsch, G. Völksch, K. Heide, Ber. Bunsenges. Phys. Chem. 100 (1996) 1438.
[37] V. M. Fokin, N. S. Yuritsyn, personal communication.
[38] P. Richet, Y. Bottinga, Earth Planet. Sci. Lett. 67 (1984) 415.
[39] D.R. Uhlmann, in: L.L. Hench, S.W. Freiman (Eds.), Advances in Nucleation and Crystallization of Glasses, Am. Ceram. Soc. Pub, Cleveland, 1972, pp. 91–115.
[40] P.D. Calvert, D.R. Uhlmann, J. Cryst. Growth 12 (1972) 291.
[41] D. Turnbull, J. Appl. Phys. 21 (1950) 1022.
[42] R. Muller, R. Naumann, S. Reinsch, Thermo. Acta 280&281 (1996) 191.
[43] V.M. Fokin, E.D. Zanotto, J.W.P. Schmelzer, J. Non-Cryst. Solids 278 (2000) 23.
[44] S. Manrich, E.D. Zanotto, Ceramica 41 (1995) 105 (in Portuguese).
[45] K.A. Jackson, Liquid Metals and Solidification, American Society for Metals, Cleveland, OH, 1958.
[46] K.A. Jackson, in: R.H. Doremus, B.W. Roberts, D. Turnbull (Eds.), Growth and Perfection of Crystals, Wiley, New York, 1958.
[47] V.O. Esin, I.P. Tarabaev, V.N. Porzkov, I.A. Vdovina, J. Cryst. Growth 66 (1984) 459.
[48] V.M. Fokin, O.V. Potapov, E.D. Zanotto, F.M. Spiandorello, V.L. Ugolkov, B.Z. Pevzner, J. Non-Cryst. Solids 331 (2003) 240.
[49] M. Roskosz, M.J. Toplis, P. Besson, P. Richet, J. Non-Cryst. Solids 3510 (2005) 1266.
[50] V.M. Fokin, personal communication, 2006.
[51] R. Müller, PhD thesis. Academy of Science of the GDR, Central Institute of Inorganic Chemistry, 1989 (in German).
[52] W. Schreyer, J.F. Schairer, Z. Kristallographie 116 (1961) 324.
[53] W. Schreyer, J.F. Schairer, J. Petrol. 2 (1961) 324.
[54] R. Mueller, T. Huebert, M. Kirsch, Silikattechn. 37 (1986) 111 (in German).
[55] X.P. Tang, U. Geyer, R. Busch, W.L. Johnson, Y. Wu, Nature 402 (1999) 160.
[56] L.W. Herron, C.G. Bergeron, Phys. Chem. Glasses 19 (5) (1978) 89.
[57] M.L.F. Nascimento, E.D. Zanotto, Phys. Chem. Glasses 48 (2007) 201.